



OPEN

SUBJECT AREAS:
GROWTH SIGNALLING
DRUG DEVELOPMENTReceived
16 May 2014Accepted
27 October 2014Published
13 November 2014Correspondence and
requests for materials
should be addressed to
R.Z. (hepatolab@163.
com)These authors
contributed equally to
this work.

A reduction in reactive oxygen species contributes to dihydromyricetin-induced apoptosis in human hepatocellular carcinoma cells

Bin Liu^{1*}, Xiaoyu Tan^{1*}, Jian Liang², Shixing Wu^{1,3}, Jie Liu¹, Qingyu Zhang¹ & Runzhi Zhu¹¹Laboratory of Hepatobiliary Surgery of Affiliated Hospital of Guangdong Medical College, Zhanjiang Key Laboratory of Hepatobiliary Diseases, Zhanjiang 524001, China, ²Department of Gastroenterology, Affiliated Hospital of Guangdong Medical College, Zhanjiang, 524001, China, ³Department of Hepatobiliary Surgery, Renmin Hospital, Hubei University of Medicine.

Reactive oxygen species (ROS) and cellular oxidant stress are considered inducers of carcinogenesis. However, the association of ROS with cancer is both complex and, at times, paradoxical. We assessed the effects of dihydromyricetin (DHM) on the induction of ROS accumulation and on the activation of the mitochondrial signaling pathway in human hepatoma HepG2 cells. The results indicated that DHM could reduce ROS accumulation in a concentration-dependent manner. Additionally, with increasing concentrations of DHM, the expression of proteins that participate in the cell apoptosis program increased in a concentration-dependent manner. Furthermore, we found that a low dose of H₂O₂ (10 nM) could reverse DHM-induced cell apoptosis. We observed the following critical issues: first, the cellular redox balance is vital in DHM-induced apoptosis of human hepatocellular carcinoma (HCC) cells, and second, ROS could function as a redox-active signaling messenger to determine DHM-induced cell apoptosis. In this study, we demonstrated that low levels of ROS are also critical for the function of HCC cells.

Dihydromyricetin (DHM, C₁₅H₁₂O₈, PubChem CID: 161557, Figure 1A) is a major active ingredient of flavonoid compounds and is a white needle-like crystal that can be extracted from *Ampelopsis grossedentata*. It exhibits potent antitumor activity against human tumors both *in vivo* and *in vitro*¹. Many other pharmacological properties have been reported for DHM, such as anti-inflammatory, antibacterial, cough suppressant, antioxidant, antihypertensive, hepatoprotective and anticancer effects^{2,3}. Recent studies have demonstrated that DHM is highly effective in counteracting acute ethanol intoxication⁴.

The implications of reactive oxygen species (ROS) regulation are highly significant for cancer therapy because ordinary antitumor drugs inhibit cancer cell proliferation through an increase in ROS. Previous studies have reported that DHM can significantly inhibit the proliferation of tumor cells⁵. In the present study, DHM abolished ROS and glutathione (GSH) production and activated caspase-9 protein in HepG2 cells in a concentration-dependent manner, which promoted cellular apoptosis. In addition, a low dose of H₂O₂ (10 nM) could reverse DHM-induced cell apoptosis. We demonstrated that the balance between ROS production and antioxidants plays a vital role in DHM-induced cell apoptosis.

Methods

Drugs and reagents. DHM (Sigma, St. Louis, MO, USA) was dissolved in 100% DMSO to prepare a 50 mM stock solution and was stored at -20°C. The final concentration of DMSO did not exceed 0.1% throughout the study. N-acetylcysteine (NAC; Sigma) was dissolved in PBS to yield a final concentration of 50 mM. Antibodies against HO-1, caspase-9, caspase-8, caspase-3, PARP, Cyt c, Bax, Bcl-2, BAK and β-actin were obtained from Cell Signaling Technology (Beverly, MA, USA). Goat anti-rabbit IgG-HRP (EarthOx, San Francisco, CA, USA) was used as a secondary antibody.

Cell culture and DHM treatment. Human hepatoma HepG2 and HL7702 cells were donated by the Clinical Research Center of the Affiliated Hospital of Guangdong Medical College (Zhanjiang, China). HepG2 and HL7702 cells were cultured in RPMI-1640 medium and DMEM, respectively, and were supplemented with 10% (v/v) fetal bovine serum (GIBCO, Invitrogen Life Technologies, Carlsbad, USA), penicillin (100 U/ml), and streptomycin (100 U/ml). The cells were maintained in a humidified atmosphere of 95% air + 5% CO₂ at 37°C. HepG2 cells were grown in standard media, and when the confluence reached 70–80%, the cells were treated with different concentrations of DHM (10, 50, or 100 μM) for 6 h, 12 h and 24 h. H₂O₂ (0, 2, 5, 10, or 50 nM) was dissolved in the medium of cells treated with 100 μM

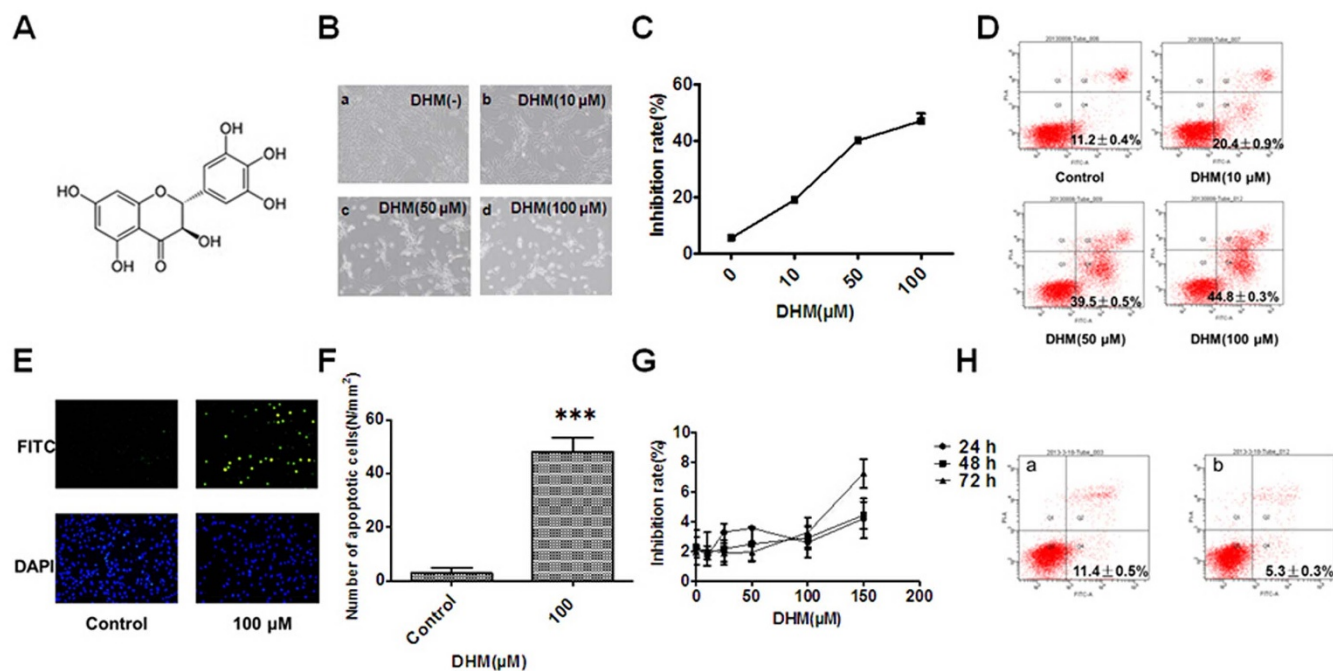


Figure 1 | DHM inhibits cell proliferation and promotes cell apoptosis. (A): The chemical structure of DHM. (B): DHM induces apoptosis in HepG2 cells at 24 h (a: control, b: 10 μM, c: 50 μM, d: 100 μM), which was visualized by microscopy ($\times 100$). (C): Cell growth, as detected by the MTT assay, was inhibited in a concentration-dependent manner at 24 h after DHM treatment. (D): DHM-induced cell apoptosis was analyzed by flow cytometry (24 h). (E): DHM-induced cell apoptosis (100 μM, DNA fragmentation) was visualized by fluorescence microscopy (24 h, TUNEL staining, original magnification: $\times 100$). (F): Number of apoptotic cells. At least six 12 mm² fields of view were counted in each culture dish. (G): DHM did not inhibit cell proliferation in normal hepatic HL7702 cells. Cell growth was detected by the MTT assay. H: HL7702 cells were treated with 100 μM DHM for 24 h, and cell apoptosis was analyzed using flow cytometry (a: Control, b: 100 μM DHM). Values are the means \pm SD for at least three independent experiments performed in triplicate.

DHM for 24 h. NAC (1 mM) was dissolved in the medium of HepG2 cells treated with 50 μM DHM. HL7702 cells were grown in standard media, and when the confluence reached 70–80%, they were treated with different concentrations of DHM (0, 5, 10, 25, 50, 100 or 150 μM) for 24 h, 48 h and 72 h.

Subcellular fractionation. Mitochondrial and cytosolic fractions of cells were prepared using a mitochondria/cytosol fractionation kit purchased from BioVision Inc. (Mountain View, CA, USA). Briefly, the cells were treated with different concentrations of DHM (0, 10, 50 or 100 μM) for 24 h and were then harvested with cold phosphate-buffered saline (PBS). Subsequently, the cells were lysed in 400 μL of extraction buffer containing dithiothreitol and protease inhibitor cocktail on ice for 30 min with homogenization using a Kontes Dounce tissue grinder (Fisher, CA, USA). After 10 min of centrifugation (700 \times g), the supernatant was centrifuged at 1200 \times g for 30 min at 4 °C. The supernatant (cytosolic fraction) was collected, and the pellets were resuspended in the mitochondrial extraction buffer (mitochondrial fraction). Nuclear and cytoplasmic fractions were prepared using a nuclear/cytosol fractionation kit purchased from BioVision Inc. according to the manufacturer's instructions.

Measurement of the intracellular level of ROS. A ROS assay kit (BioVision) was used to detect the accumulation of intracellular ROS in HepG2 cells. Briefly, cells were treated with different concentrations of DHM (0, 10, 50 or 100 μM) for 6 h, 12 h and 24 h and were subsequently cultured with or without 10 nM H₂O₂ for 24 h. After removing the medium containing 100 μM DHM, 100 μL of DCFDA mix containing 2.5 \times 10⁴ cells was added to each well and incubated for 45 min at 37 °C in the dark. Blank wells (with non-stained cells) were also used as a control. The fluorescence intensity was measured using a fluorescence plate reader (EnSpire™ 2300 Multilabel Reader, PE) at Ex/Em. = 488/525 nm.

Measurement of intracellular GSH levels. The intracellular level of GSH was determined using an ApoGSH glutathione detection kit (BioVision) according to the manufacturer's instructions. Briefly, after treating cells with different concentrations of DHM (0, 10, 50 or 100 μM) for 6 h, 12 h and 24 h, 1 \times 10⁶ cells were harvested and centrifuged at 700 \times g for 5 min. The cells were then lysed in 100 μL of ice-cold lysis buffer on ice for 10 min and centrifuged at 1200 \times g for 10 min at 4 °C. The supernatant was then analyzed with the glutathione detection kit. The fluorescence was measured using a fluorescence plate reader (EnSpire™ 2300 Multilabel Reader, PE) at Ex/Em. = 380/460 nm.

Measurement of ATP production. The intracellular level of ATP was measured using an ApoSENSOR cell viability assay kit (BioVision) according to the manufacturer's instructions. Briefly, cells were treated with DHM (10, 50 or 100 μM) for 6 h, 12 h and 24 h. Subsequently, 10⁴ cells were incubated with 100 μL of nuclear releasing reagent for 5 min at room temperature with gentle shaking, followed by further incubation with 4 μL of ATP monitoring enzyme. Detection was performed using a luminometer (Berthold Sirius L, Germany).

Annexin V/PI double staining assay. Apoptotic cells were quantified using an Annexin V-FITC/PI kit (BioVision), detected by flow cytometry (FACSCalibur, Becton Dickinson), and analyzed with Modfit and CellQuest software (BD Biosciences, Franklin Lakes, NJ, USA). Briefly, NAC (1 mM) was dissolved in the medium of HepG2 cells treated with 50 μM DHM. HL7702 cells were treated with 100 μM DHM for 24 h. HepG2 cells were either pretreated with 50, 100 and 150 μM DHM and subsequently incubated with 1 mM NAC or pretreated with 50 μM DHM and subsequently incubated with 10 nM H₂O₂. Experiments were performed for 24 h or 12 h. Then, the cells were collected and resuspended in binding buffer (pH 7.5, 10 mM HEPES, 2.5 mM CaCl₂ and 140 mM NaCl) and incubated with Annexin V-FITC and PI for 10 min in the dark prior to flow cytometric analysis. Cells that were in early stages of apoptosis were Annexin V-positive, whereas Annexin V and PI double-positive cells were considered to be in the late stages of apoptosis.

TUNEL staining assay. Apoptotic cells were detected using a DeadEnd™ Fluorometric TUNEL System kit (Promega, USA). Briefly, cell densities were adjusted to 2 \times 10⁴ cells per 100 μL. The cells were seeded into a 96-well plate, which was kept in an incubator overnight to allow for attachment and recovery, pretreated with 100 μM DHM for 24 h and washed twice. The cells were then fixed in freshly prepared 4% methanol-free formaldehyde solution in PBS (pH 7.4) for 25 min at 4 °C, permeabilized with 0.2% Triton® X-100 solution in PBS for 5 min and stained with 40 mL of DAPI solution for 15 min at room temperature in the dark. The samples were analyzed using a fluorescence microscope (OLYMPUS, IX70, Japan) equipped with a standard fluorescein filter set to view green fluorescence at 520 \pm 20 nm and blue fluorescence (for DAPI) at 460 nm.

MTT assay. HepG2 and HL7702 cell densities were adjusted to 2 \times 10⁴ cells per 100 μL. The cells were seeded into a 96-well plate, which was kept in an incubator overnight to allow for attachment and recovery. HepG2 cells were pretreated with 10, 50 or 100 μM DHM for 6 h, 12 h and 24 h. HL7702 cells were pretreated with 5, 10, 25, 50, 100 or 150 μM DHM for 24 h, 48 h or 72 h. HepG2 cells were pretreated with



50 μM DHM and subsequently treated with H_2O_2 (2, 5, 10, 50 or 100 nM) for 24 h. MTT was dissolved in warm assay medium to a concentration of 5 mg/mL. A total of 20 μL of MTT solution was transferred to each well to yield a final volume of 120 μL /well. The plates were incubated for 4 h at 37°C with 5% CO_2 . Then, the supernatants were removed, and 100 μL of DMSO was added to ensure total solubility of the formazan crystals. After 15 min of shaking, the absorbance was measured at 490 nm using a plate reader (Perkin-Elmer, Waltham, USA). The inhibition ratio (%) was calculated using the following equation:

$$\text{Inhibition ratio (100\%)} = [1 - \text{OD}_{490} (\text{DHM-treated cells}) / \text{OD}_{490} (\text{Control})] \times 100\%$$

Analysis of DHM-regulated apoptotic proteins. Cells were collected after treatment and were then lysed in lysis buffer (100 mM Tris-HCl, pH 6.8, 4% (m/v) sodium dodecyl sulfate (SDS), 20% (v/v) glycerol, 200 mM 2-mercaptoethanol, 1 mM phenylmethyl sulfonyl fluoride, and 1 $\mu\text{g}/\text{mL}$ aprotinin) for 30 min on ice. The lysate was separated by centrifugation at 4°C for 15 min at 1200 $\times g$. The total protein concentration in the supernatant was detected using a BCA protein assay kit (Beyotime Institute of Biotechnology, Haimen, Jiangsu, China). SDS-PAGE was performed with an 8–15% gradient or with standard polyacrylamide gels. Proteins were then transferred to nitrocellulose membranes, which were saturated with 5% milk in TBST (Tris-buffered saline and 1% Tween 20) and incubated with primary antibodies in diluent overnight at 4°C. The membranes were washed three times with TBST and were incubated with goat anti-rabbit IgG-HRP secondary antibody for 1 h, followed by four washes with TBST. Detection was performed using an Odyssey Infrared Imaging System (LI-COR Inc., NE).

Cells were incubated for 6 h with or without DHM. All floating and attached cells were harvested, fixed with ice-cold 4% paraformaldehyde for 10 min and washed with ice-cold PBS. Then, the cells were permeabilized with 0.3% Triton X-100, washed with ice-cold PBS, stained with antibodies against Cyt c and AIF and subsequently incubated with Alexa Fluor secondary antibodies (Invitrogen, California, USA). After the cell nuclei were stained with DAPI, the cells were observed using a fluorescence microscope (CS SP5II, Germany) with peak excitation wavelengths of 555 nm, 645 nm and 460 nm.

Statistical analysis. All results shown represent the mean \pm SD of triplicate experiments performed in a parallel manner unless otherwise indicated. The results were evaluated using Student's *t*-test, and differences were considered significant at the * $P < 0.05$, ** $P < 0.01$ or *** $P < 0.001$ level. All figures shown in this paper are representative of at least three independent experiments.

Results

DHM inhibits proliferation and promotes apoptosis in HepG2 cells. Untreated HepG2 cells grew well, whereas the cells treated with DHM for 24 h were distorted in shape, and most became round (Figure 1B); in addition, the number of sloughed cells increased in a concentration-dependent manner. An MTT assay was used to evaluate the inhibitory effects of DHM on HepG2 cells. DHM treatment of HepG2 cells resulted in significant concentration-dependent inhibition of cell growth at 24 h (Figure 1C). These data revealed that DHM strongly reduced the viability of HepG2 cells, which may contribute to its antitumor potency. Cells that were treated with 50 μM DHM were distorted in shape and floated in the medium; cell growth was inhibited, and most HepG2 cells underwent apoptosis. The apoptosis occurred in a concentration-dependent manner for 24 h (Figure 1D). TUNEL staining was used to detect cell death, and the results showed that the amount of DNA fragmentation in cells that were treated with 100 μM DHM was much higher than that in vehicle-treated cells at 24 h (Figure 1E and F); this was evidenced by an increase in green fluorescence. These results demonstrated that DHM could significantly inhibit proliferation and could promote apoptosis of HepG2 cells in a concentration-dependent manner. By contrast, the normal hepatic HL7702 cell line was not sensitive to DHM (Figure 1G and H).

DHM sharply reduces ROS production in HepG2 cells. We measured the ROS level in HepG2 cells that were treated with various concentrations of DHM for 6 h, 12 h and 24 h. The cellular oxidation of H₂DCFDA, which is oxidized to green fluorescent DCF by various peroxide-like ROS and by nitric oxide-derived reactive intermediates, was used as a probe. The data demonstrated that DHM could significantly decrease the production of ROS to a very low level in HepG2 cells and that the imbalance of ROS may promote mitochondrial dysfunction and

trigger mitochondria-mediated apoptosis. The intracellular levels of ROS in cells treated with 10, 50 and 100 μM DHM decreased in a concentration-dependent manner compared with the levels in vehicle-treated cells (Figure 2A-a).

DHM markedly reduces the level of GSH in HepG2 cells. We used monochlorobimane (MCB) dye to detect the levels of GSH in HepG2 cells that were treated with various concentrations of DHM for 6 h, 12 h and 24 h. The unbound form of MCB is almost non-fluorescent, whereas it fluoresces blue (Ex/Em. = 380/460 nm) when bound to GSH. The data revealed that DHM could significantly decrease the production of GSH in HepG2 cells, which may promote mitochondrial dysfunction and trigger mitochondria-mediated apoptosis. Intracellular levels of GSH in cells treated with 10, 50 and 100 μM DHM decreased in a concentration-dependent manner compared with the levels in vehicle-treated cells (Figure 2A-b).

DHM reduces the intracellular level of ATP in HepG2 cells. To evaluate the dysfunction in mitochondrial energy production, we detected the intracellular levels of ATP in DHM-treated cells. Cells were treated with various concentrations of DHM for 6 h, 12 h and 24 h, and the data indicated that the intracellular levels of ATP dramatically decreased in a concentration-dependent manner (Figure 2A-c).

DHM regulates the production of apoptotic proteins. The loss of ROS induces cell apoptosis through the release of proapoptotic proteins such as Cyt c, which are released from the mitochondria into the cytosol⁶. In the present study, cells were treated with 100 μM DHM for 6 h, and it was found that Cyt c was released from the mitochondria into the cytosol (white arrow) (Figure 2B-a, c), whereas AIF was not detected in the nucleus (Figure 2B-b, d). Cyt c can activate caspase-9, which in turn activates caspase-3 via the induction of cleavage. Poly ADP-ribose polymerase (PARP), an important substrate of caspase-3, can then be cleaved. In the present study, cells were treated with different concentrations of DHM for 24 h. Increases in activated caspase-9, caspase-8 and caspase-3 were observed. The results showed that the expression of caspase-9 and caspase-3 were increased and that the levels of cleaved PARP were elevated in DHM-treated HepG2 cells compared with controls. The oxidative stress-related protein HO-1 and BAK were increased whereas Bcl-2 was decreased in a concentration-dependent manner; however, no changes were observed in the levels of Bax (Figure 2C).

A low dose of H_2O_2 reversed DHM-induced cell apoptosis. To confirm whether cells that were treated with DHM could be rescued with H_2O_2 , HepG2 cells were co-cultured with 100 μM DHM and H_2O_2 (2, 5, 10, 50 and 100 nM) for 24 h. We found that very few HepG2 cells that were co-cultured with 100 μM DHM and 10 nM H_2O_2 underwent apoptosis. (The data did not shown). In HepG2 cells that were treated with 100 μM DHM for 24 h and cultured with fresh culture medium containing 10 nM H_2O_2 , it was observed that minimal cell apoptosis was observed, and normal cell growth was recovered 24 h after DHM withdrawal (Figure 3A-a). An annexin V/PI double-staining assay was used to evaluate the apoptotic activity of HepG2 cells. This assay demonstrated that the rate of apoptosis of cells treated with 10 nM H_2O_2 was decreased compared with that of cells treated with vehicle (Figure 3A-b). A micro-dose of H_2O_2 could reverse DHM-induced cell apoptosis, and the production of ROS was reduced 24 h after DHM withdrawal; however, ROS production recovered to a greater extent with a micro-dose of H_2O_2 (Figure 3A-c).

NAC exacerbates DHM-mediated ROS reduction in HepG2 cells. To illustrate the role of ROS in DHM-induced apoptosis, HepG2 cells were treated with DHM in the presence or absence of the

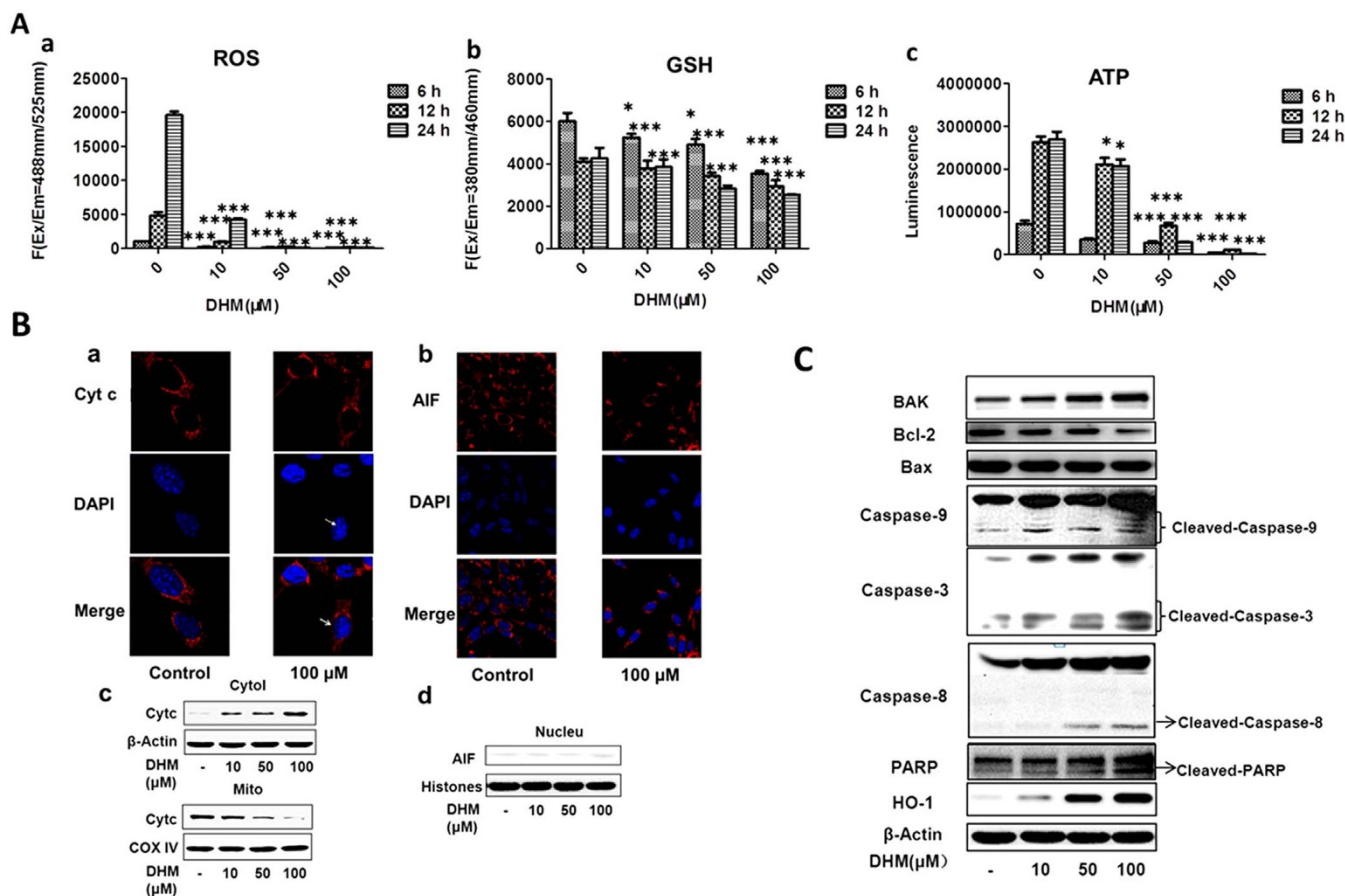


Figure 2 | DHM reduced ROS, GSH and ATP production in HepG2 cells, and DHM regulated apoptotic proteins in HepG2 cells in a concentration-dependent manner. (A): Cells were treated with DHM (10, 50 and 100 μM) for 6 h, 12 h and 24 h, and then intracellular levels of ROS (a), GSH (b) and ATP (c) were detected. The intracellular levels of ROS, GSH and ATP in DHM-treated cells were markedly decreased compared with their levels in the vehicle control. (B): The cells were immunostained with anti-Cyt c (a) and anti-AIF (b) together with DAPI nuclear staining. Cells were treated with 100 μM DHM for 6 h and were visualized using confocal microscopy. (c): Cyt c protein expression in the mitochondria and cytosol; the release of Cyt c from the mitochondria to the cytosol is illustrated. (d): AIF protein was not detected in the nucleus. (C): Cells were treated with DHM (10, 50 and 100 μM) for 24 h, and the levels of PARP, caspase-9, caspase-3, caspase-8, HO-1, Bcl-2, BAK and Bax proteins were detected by western blotting in HepG2 cells. The data showed that DHM regulates apoptotic proteins in HepG2 cells in a concentration-dependent manner. All images are representative of three independent experiments. Values are the means \pm SD for at least three independent experiments performed in triplicate. * $P < 0.05$, ** $P < 0.01$ and *** $P < 0.001$ indicate significant differences between the experimental and control groups.

antioxidant NAC. The results showed that NAC exacerbated the DHM-mediated reduction of ROS and induced more apoptosis in HepG2 cells (Figure 3B, C).

Discussion

In the present study, our results showed that DHM could induce apoptosis in HepG2 cells. As the concentration of the drug increased, cell proliferation decreased, and the rate of apoptosis increased. However, DHM did not inhibit cell growth in normal hepatic HL7702 cells. Historically, ROS have been considered to lack specific functions beyond causing cell damage and physiological dysfunction. The accumulation of ROS has been linked to multiple pathologies, including neurodegenerative diseases, cancer, and premature aging⁷. Previous studies have considered that ROS are a “by-product” of cellular aerobic metabolism and cytotoxicity. However, recent studies suggest that low levels of ROS could function as redox-active signaling messengers to promote the proliferation and differentiation of cells. Thus, intracellular ROS may not be a “by-product” but rather an important class of signaling molecules involved in multiple signaling pathways for cellular proliferation and differentiation^{8–11}. The demand for ROS in cancer cells is higher than that in normal cells. If the content of ROS is lower than the minimum requirement

for a cellular response, cancer cells would not grow normally¹². In this study, we confirmed that a sharp decline in the production of ROS could significantly inhibit cell proliferation and induce apoptosis of HepG2 cells.

Many chemical and physiological phenomena that are capable of inducing apoptosis are known to provoke oxidative stress via the generation of ROS, which suggests a close relationship between oxidative stress and apoptosis^{13,14}. H_2O_2 may directly induce apoptosis, whereas antioxidants could block this effect¹⁵. In the present study, we found that treatment with DHM significantly induced apoptosis in HepG2 cells; however, apoptosis could be reversed with a low dose of H_2O_2 . These results suggest that the balance between ROS production and antioxidants could regulate DHM-induced early and late apoptosis in HepG2 cells. Our results indicated that the balance between ROS production and various antioxidants was very important for the growth of cancer cells. DHM sharply reduced the production of ROS in HepG2 cells, which might have disrupted the balance of redox reactions. This disruption occurred in a concentration-dependent manner. DHM thus disturbed the cells’ internal balance and blocked ROS-mediated signal transduction to induce tumor cell apoptosis. However, its mechanism of action has not been clearly defined.

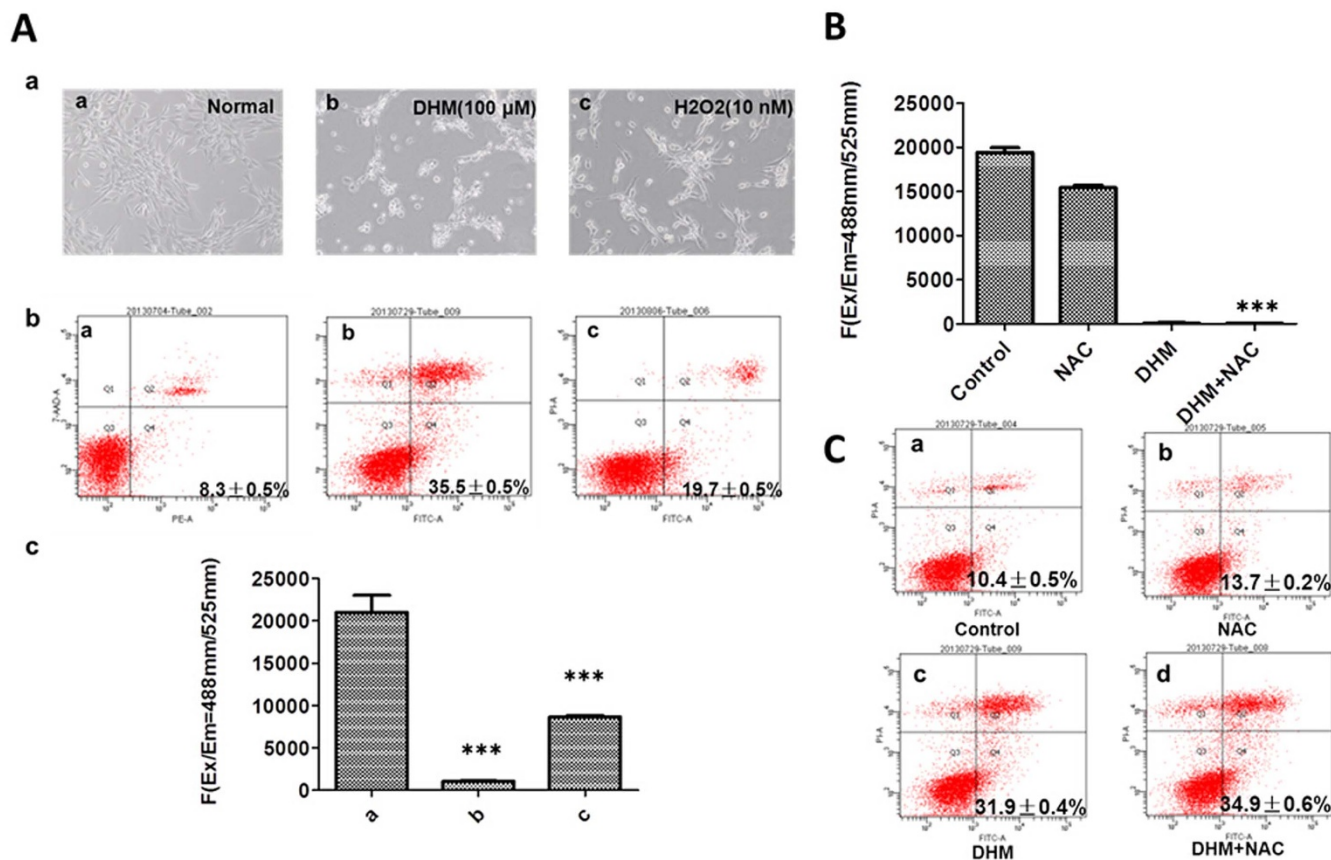


Figure 3 | A low dose of H_2O_2 reversed DHM-induced apoptosis, whereas NAC aggravated DHM-induced apoptosis. (A): a: DHM-induced apoptosis in HepG2 cells with or without H_2O_2 (a: normal HepG2 cells, b: HepG2 cells cultured for 24 h after withdrawal of 100 μM DHM, c: HepG2 cells cultured with 10 nM H_2O_2 for 24 h after withdrawal of 100 μM DHM). The cells were visualized by microscopy ($\times 100$). b: Apoptosis was analyzed according to flow cytometry distributions (a: normal HepG2 cells, b: HepG2 cells cultured for 24 h after withdrawal of 100 μM DHM, c: HepG2 cells cultured with 10 nM H_2O_2 for 24 h after withdrawal of 100 μM DHM). c: ROS production was measured for the treatment described in b. B: Cells were pretreated with 1 mM NAC for 1 h and subsequently treated with or without 50 μM DHM for 24 h; intracellular ROS levels were then measured. The intracellular levels of ROS decreased in the DHM-NAC-treated cells compared with the NAC-treated cells. C: Apoptosis was analyzed according to the flow cytometry distributions for the treatments in B (a: normal HepG2 cells, b: NAC pretreatment, c: DHM without NAC pretreatment, d: DHM with NAC pretreatment). The values are the means \pm SD for at least three independent experiments performed in triplicate. * $P < 0.05$, ** $P < 0.01$ and *** $P < 0.001$.

In recent years, the term “redox state” has not only been used to describe a physiologically balanced redox state, such as GSSG/GSH, but has also been used to describe a general cellular oxidation/reduction environment¹⁶. Under normal conditions, a cell’s redox state is maintained within a narrow range similar to the manner in which a biological system regulates its pH. Under pathological conditions, the redox state can be altered to lower or higher values¹⁷. Low GSH levels are associated with mitochondrial dysfunction and cell apoptosis, which could reduce the chemoresistance of tumors¹⁸. Our data indicated that DHM significantly reduced the production of GSH in HepG2 cells. Moreover, ATP acts as a direct energy source for cellular metabolism, and the amount of ATP might be directly influenced by the process of apoptosis. As cells proliferate, intracellular ROS, ATP and GSH are also gradually increased (Figure 2A-a, b, c). Our results showed that DHM dramatically decreased the level of GSH and the generation of ATP in a concentration-dependent manner. Heme oxygenase-1 (HO-1) is a widespread and redox-sensitive enzyme that catabolizes heme to carbon monoxide (CO), iron, and biliverdin. A battery of redox-sensitive transcription factors, such as activator protein-1 (AP-1), nuclear factor-kappa B (NF- κ B) and nuclear factor E2-related factor-2 (Nrf2), and their upstream kinases, including mitogen-activated protein kinases, play an important regulatory role in HO-1 gene induction¹⁹. In many tissues and in various mammalian species, the induction of HO-1 mRNA has served as a useful marker

of cellular oxidative stress²⁰. HO-1 is usually expressed at low levels under normal conditions, but it is highly induced in response to various reagents that cause oxidative stress, including ultraviolet irradiation, hydrogen peroxide, heavy metals, and lack of oxygen. HO-1 has been assumed to play a role in the induction of chemotherapeutic protective mechanisms^{21,22}. Our results also demonstrated that up-regulation of HO-1 expression induced by DHM could lead to apoptosis in HepG2 cells in a concentration-dependent manner.

We performed immunofluorescence and western blot analysis of cytochrome c and AIF in HepG2 cells. Our findings provide a paradigm for mitochondria-dependent cell death pathways that involve a postmitochondrial level of pharmacological and possibly endogenous regulation that precedes the intracytosolic release of the caspase-independent death effector AIF. We did not observe AIF production in the nucleus, but we found that Cyt c released from mitochondria exerted its apoptogenic effects in the cytosol through its role in caspase-8 and caspase-9 activation. As a substrate of caspase-9, PARP is involved in repairing DNA damage. During apoptosis, the activation of caspase-9 is a crucial step in apoptotic cell death^{23–25} because it induces PARP cleavage. PARP is proposed to be important in the control of many cellular processes, such as DNA repair, cell death, chromatin function and maintenance of genome stability²⁶. PARP activation is an early DNA damage response indicator. Previous studies have demonstrated that cell survival is maintained if Bcl-2

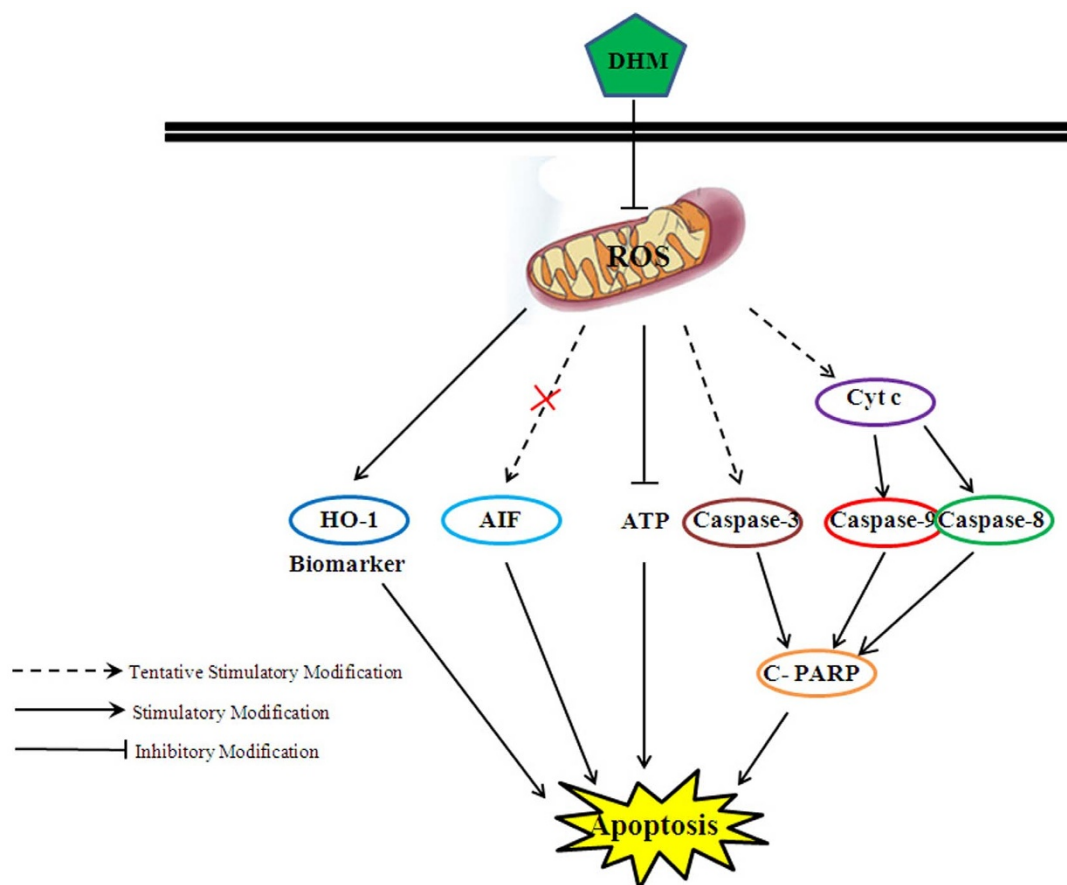


Figure 4 | Cellular pathway of DHM-induced cell apoptosis in HepG2 cells. DHM induced HepG2 cell apoptosis via the activation of Cyt c, caspase-9 and PARP; moreover, the production of ROS decreased, which eventually led to apoptosis.

and Bax are balanced and that a higher Bcl-2 expression level leads to inhibition of apoptosis^{27,28}. In this study, we confirmed that DHM could elevate the levels of caspase-9 and cleaved PARP proteins in the HepG2 cell line, whereas the levels of PARP and Bcl-2 proteins decreased. However, DHM had no effect on the release of AIF. These data suggest that the loss of ROS-mediated signaling may promote apoptosis in human hepatoma cells.

The main ROS species are superoxide and hydrogen peroxide, both of which are redox signaling molecules in the context of various cellular functions. Redox imbalance due to excessive or insufficient ROS is an induction factor for the pathogenesis of disease, including cancer development and progression. We confirmed that ROS is significantly associated with cell growth and that loss of ROS could trigger activation of caspase-9 and cleavage of PARP, leading to apoptosis. In this study, we found that apoptosis that was induced by DHM could be reversed by a small amount of accumulated ROS. We confirmed that cellular redox balance plays a vital role in carcinogenesis. We consider the formation of ROS to be a requisite and beneficial event for cancer cell growth, and we hypothesize that an imbalance in redox reactions could result in tumor cell death (Figure 4). Although future investigations should be conducted to demonstrate the molecular mechanism underlying the DHM-induced reduction of ROS generation, our data indicated that DHM-induced apoptosis may act, at least partially, through a ROS-related pathway in hepatocellular carcinoma HepG2 cells.

- Li, H. *et al.* Comparison of refluxing, ultrasonic- and microwave-assisted extraction of dihydromyricetin from *Ampelopsis grossedentata*. *J AOAC Int* **91**, 1278–1283 (2008).
- Ye, J., Guan, Y., Zeng, S. & Liu, D. Ampelopsin prevents apoptosis induced by H₂O₂ in MT-4 lymphocytes. *Planta Med* **74**, 252 (2008).

- Kundaković, T. *et al.* Cytotoxic, antioxidant, and antimicrobial activities of *Ampelopsis brevipedunculata* and *Parthenocissus tricuspidata* (Vitaceae). *Arch Biol Sci* **60**, 641–647 (2008).
- Shen, Y. *et al.* Dihydromyricetin as a novel anti-alcohol intoxication medication. *J Neurosci* **32**, 390–401 (2012).
- Sosa, V. *et al.* Oxidative stress and cancer: An overview. *Ageing Res Rev* **12**, 376–390, doi:10.1016/j.arr.2012.10.004 (2012).
- Circu, M. L. & Aw, T. Y. Reactive oxygen species, cellular redox systems, and apoptosis. *Free Radical Bio Med* **48**, 749–762 (2010).
- Sena, L. A. & Chandel, N. S. Physiological roles of mitochondrial reactive oxygen species. *Mol cell* **48**, 158–167, doi:10.1016/j.molcel.2012.09.025 (2012).
- Zhu, R., Wang, Y., Zhang, L. & Guo, Q. Oxidative stress and liver disease. *Hepatol Res: the official journal of the Japan Society of Hepatology* **42**, 741–749, doi:10.1111/j.1872-034X.2012.00996.x (2012).
- Emerling, B. M. *et al.* Hypoxic activation of AMPK is dependent on mitochondrial ROS but independent of an increase in AMP/ATP ratio. *Free Radical Bio Med* **46**, 1386–1391 (2009).
- Hernandez-Garcia, D., Wood, C. D., Castro-Obregon, S. & Covarrubias, L. Reactive oxygen species: A radical role in development? *Free Radical Bio Med* **49**, 130–143, doi:10.1016/j.freeradbiomed.2010.03.020 (2010).
- Khan, A. Q., Nafees, S. & Sultana, S. Perillyl alcohol protects against ethanol induced acute liver injury in Wistar rats by inhibiting oxidative stress, NFkappa-B activation and proinflammatory cytokine production. *Toxicology* **279**, 108–114, doi:10.1016/j.tox.2010.09.017 (2011).
- Trachootham, D., Alexandre, J. & Huang, P. Targeting cancer cells by ROS-mediated mechanisms: a radical therapeutic approach? *Nat Rev Drug Discov* **8**, 579–591 (2009).
- Pathak, N. & Khandelwal, S. Oxidative stress and apoptotic changes in murine splenocytes exposed to cadmium. *Toxicology* **220**, 26–36 (2006).
- Halliwell, B. & Gutteridge, J. Role of free radicals and catalytic metal ions in human disease: an overview. *Method Enzymol* **186**, 1–85 (1989).
- Zhang, L. *et al.* Heat shock transcription factor-1 inhibits H₂O₂-induced apoptosis via down-regulation of reactive oxygen species in cardiac myocytes. *Mol Cell Bio* **347**, 21–28 (2011).
- Flohé, L. Glutathione Peroxidases. *Selenoproteins and Mimics*, 1–25 (2012).
- Buonocore, G., Perrone, S. & Tataranno, M. L. in *Semin in Fetal Neonat M.* 186–190 (Elsevier).



18. Nie, F. *et al.* Reactive oxygen species accumulation contributes to gambogic acid-induced apoptosis in human hepatoma SMMC-7721 cells. *Toxicology* **260**, 60–67 (2009).
19. Yi, L. *et al.* Heme regulatory motifs in heme oxygenase-2 form a thiol/disulfide redox switch that responds to the cellular redox state. *J Bio Chem* **284**, 20556–20561 (2009).
20. McDonald, J. T. *et al.* Ionizing radiation activates the Nrf2 antioxidant response. *Cancer Res* **70**, 8886–8895 (2010).
21. Stapleton, P. A., Goodwill, A. G., James, M. E., Brock, R. W. & Frisbee, J. C. Hypercholesterolemia and microvascular dysfunction: interventional strategies. *J Inflammation* **7**, 54 (2010).
22. Soares, M. P. & Bach, F. H. Heme oxygenase-1: from biology to therapeutic potential. *Trends Mol Med* **15**, 50–58 (2009).
23. Allan, L. A. & Clarke, P. R. Apoptosis and autophagy: Regulation of caspase-9 by phosphorylation. *FEBS J* **276**, 6063–6073 (2009).
24. Bratton, S. B. & Salvesen, G. S. Regulation of the Apaf-1–caspase-9 apoptosome. *J Cell Sci* **123**, 3209–3214 (2010).
25. Yasuda, Y., Saito, M., Yamamura, T., Yaguchi, T. & Nishizaki, T. Extracellular adenosine induces apoptosis in Caco-2 human colonic cancer cells by activating caspase-9/-3 via A_{2a} adenosine receptors. *J Gastroenterology* **44**, 56–65 (2009).
26. Peralta-Leal, A. *et al.* PARP inhibitors: new partners in the therapy of cancer and inflammatory diseases. *Free Radical Bio Med* **47**, 13–26, doi:10.1016/j.freeradbiomed.2009.04.008 (2009).
27. Nagoor, N. H. 7 alpha-Hydroxy-beta-Sitosterol from *Chisocheton tomentosus* Induces Apoptosis via Dysregulation of Cellular Bax/Bcl-2 Ratio and Cell Cycle Arrest by Downregulating ERK1/2 Activation. *Evid-Based Compl Alt* **2012** (2012).
28. Del Poeta, G. *et al.* The genotype nucleophosmin mutated and FLT3-ITD negative is characterized by high bax/bcl-2 ratio and favourable outcome in acute myeloid leukaemia. *Brit J Haematol* **149**, 383–387 (2010).

Acknowledgments

This work was supported in part by the following grants: Guangdong medical college scientific research fund (No. Q2012033, M2013012 and M2013024), China; The second batch of 2013 Zhanjiang financial special backup project of science and technology (No. 10). This work was also supported by the Institute of Neurology, Affiliated Hospital of Guangdong Medical College. We thank Dr. Du Feng, Wen Li, Wenxian Wu, Weili Tian, and Xingli Zhang.

Author contributions

R.Z.Z. wrote the article. B.L. and X.Y.T. performed the experiments. J.L. (The third author), S.X.W., J.L. and Q.Y.Z. prepared Figures 1–4. B.L. participated in data and statistical analyses. All authors reviewed the final version of the manuscript.

Additional information

Competing financial interests: The authors declare no competing financial interests.

How to cite this article: Liu, B. *et al.* A reduction in reactive oxygen species contributes to dihydromyricetin-induced apoptosis in human hepatocellular carcinoma cells. *Sci. Rep.* **4**, 7041; DOI:10.1038/srep07041 (2014).



This work is licensed under a Creative Commons Attribution-NonCommercial-NoDerivs 4.0 International License. The images or other third party material in this article are included in the article's Creative Commons license, unless indicated otherwise in the credit line; if the material is not included under the Creative Commons license, users will need to obtain permission from the license holder in order to reproduce the material. To view a copy of this license, visit <http://creativecommons.org/licenses/by-nc-nd/4.0/>



DOI: 10.1038/srep07940

SUBJECT AREAS:
GROWTH FACTOR
SIGNALLING
DRUG DEVELOPMENT

ERRATUM: A reduction in reactive oxygen species contributes to dihydromyricetin-induced apoptosis in human hepatocellular carcinoma cells

Bin Liu, Xiaoyu Tan, Jian Liang, Shixing Wu, Jie Liu, Qingyu Zhang & Runzhi Zhu

SCIENTIFIC REPORTS:
4 : 7041
DOI: 10.1038/srep07041
(2014)

The original version of this Article contained a typographical error in the spelling of the author Bin Liu which was incorrectly given as Bin Lin. This has now been corrected in both the PDF and HTML versions of the Article.

Published online
13 November 2014

Updated:
15 January 2015